ACS APPLIED MATERIALS & INTERFACES

Letter

www.acsami.org

One-Dimensional Surface-Imprinted Polymeric Nanotubes for Specific Biorecognition by Initiated Chemical Vapor Deposition (iCVD)

Gozde Ozaydin Ince,*[,†] Efe Armagan,[†] Hakan Erdogan,[‡] Fatih Buyukserin,[§] Lokman Uzun,[⊥] and Gokhan Demirel*[,‡]

[†]Faculty of Engineering and Natural Sciences, Sabanci University, 34956 Istanbul, Turkey

[‡]Bio-inspired Materials Research Laboratory (BIMREL), Department of Chemistry, Gazi University, 06500 Ankara, Turkey

[§]Department of Biomedical Engineering, TOBB University of Economics and Technology, 06560 Ankara, Turkey

[⊥]Department of Chemistry, Hacettepe University, 06800 Ankara, Turkey

Supporting Information

ABSTRACT: Molecular imprinting is a powerful, generic, and cost-effective technique; however, challenges still remain related to the fabrication and development of these systems involving nonhomogeneous binding sites, insufficient template removing, incompatibility with aqueous media, low rebinding capacity, and slow mass transfer. The vapor-phase deposition of polymers is a unique technique because of the conformal nature of coating and offers new possibilities in a number of applications including sensors, microfluidics, coating, and bioaffinity platforms. Herein, we demonstrated a simple but versatile concept to generate one-dimensional surface-imprinted polymeric nanotubes within anodic aluminum oxide (AAO) membranes based on initiated chemical vapor deposition (iCVD) technique for biorecognition of immunoglobulin G (IgG). It is reported that the fabricated surface-imprinted nanotubes showed high binding capacity and significant specific recognition ability toward target molecules compared with the nonimprinted forms. Given its simplicity and universality, the iCVD method can offer new possibilities in the field of molecular imprinting.

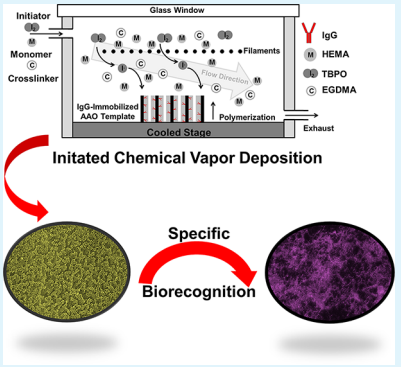

KEYWORDS: *molecular imprinting, anodic aluminum oxide (AAO), initiated chemical vapor deposition (iCVD), biorecognition, polymeric nanotube, immunoglobulin G (IgG)*

INTRODUCTION

Molecular imprinting (MI) is an emerging and promising technology for the specific molecular recognition. In molecular imprinting, polymer matrices with specific binding sites for a target molecule are prepared using monomers with functional groups. The monomers are arranged around a template, which is the target molecule to be detected, and form covalent or noncovalent bonds with the template. Polymerization of the monomers with a cross-linker leads to a polymer network keeping the functional groups in position. The template is then removed, leaving behind a cavity with highly specific receptor sites for rebinding of target molecules.[1,2] Recently, molecularly imprinted materials, especially polymers, have received growing attention because of their chemical and mechanical stabilities, low costs, high selectivities toward target molecules, and ease of fabrications for possible applications in catalysis, drug release, sensors, and separations.[3−5] So far, different approaches have been reported for the fabrication of molecularly imprinted materials involving nanosphere lithography,[6] cryogelation,[7] sol−gel synthesis,[8] template-based approaches,[9] living polymerization,[10] and block copolymer self-assembly.[11] In spite of the advances in the field of MI, there are still challenges related to the template size, conformational flexibility, heterogeneous binding sites, poor site accessibility, template leakage, incompatibility with aqueous media, low rebinding capacity, and slow mass transfer.[3,4] Therefore, development of new materials and fabrication techniques are still crucial to solving these problems.

The vapor-phase deposition of polymers is a solvent-free, environmentally friendly, and material-independent method and offers unique advantages compared to solvent-based polymerization techniques.[12−14] By applying this method, for example, nonplanar substrate geometries can be conformally coated, and unwanted impurities, degradation of the underlying layer, and changes in the mechanical/chemical properties associated with the use of solvents can be precisely eliminated.[13,15] Initiated chemical vapor deposition (iCVD) is a special class of vapor-phase polymerization techniques that is based on free radical polymerization.[15,16] In a typical iCVD process, monomer and initiator vapors are delivered into a

Received: May 10, 2013
Accepted: June 27, 2013
Published: June 27, 2013

 © 2013 American Chemical Society dx.doi.org/10.1021/am401769r | ACS Appl. Mater. Interfaces 2013, 5, 6447−6452

vacuum reactor with pressure in mTorr ranges. Initiator molecules are first thermally decomposed by hot filaments that result in the formation of free radicals. Because of the relatively low temperatures of the filaments (~150−300 °C, below the decomposition temperature of the monomer) the monomer molecules are not affected by the filament and, thus, adsorb on the substrate with the functional groups remaining intact.[15] The free radicals then attack the double bonds of adsorbed monomers creating the monomer radicals. Polymerization reaction is then propagated and terminated similar to the liquid phase. Polymerization takes place on the substrate surface, enabling the deposition of highly cross-linked polymers which are not soluble in solvents. Furthermore, because of the solventless nature of the iCVD technique, the pores of the AAO membranes can be conformally coated. Given its simplicity and ability to fabricate polymeric thin films on any substrate, iCVD technique has been utilized for a number of applications including microfluidic, tissue engineering, sensing, photovoltaic, organic electronic, and drug release.[15,17−20] However, to the best of our knowledge, its use for the surface imprinting of biological molecules has never been demonstrated.

In this work, we introduced, for the first time, a simple yet facile method for the generation of one-dimensional surface-imprinted polymeric nanotubes. First, the template biomolecules (IgG in our case) were chemically linked to the nanopores of anodic aluminum oxide (AAO) membrane. The polymerization of poly(2-hydroxyethyl methacrylate) [PHEMA] was then carried out into the IgG conjugated pores via iCVD method. Following polymerization, template biomolecules and AAO membrane were removed leaving one-dimensional polymeric nanotubes having specific IgG recognition sites situated at their surfaces.

The method described in this work combines the molecular imprinting concept with the vapor-phase polymer deposition method. The solventless nature of the iCVD polymerization method enables the usage of solvent-sensitive target molecules or polymers. Furthermore, it gives us the freedom to choose from a wide range of highly cross-linked polymers, which are insoluble in solvents, to be used as the polymer matrix. The vapor-based nature of iCVD enables the fabrication of imprinted nanostructures with various shapes tailored for specific applications. In this work, imprinted hollow nanotubes were fabricated using AAO membranes and iCVD method to deposit in the pores of the membranes. The nanotubes, compared to their bulk counterparts, have significantly larger surface area making them better alternatives to be used in sensors. The imprinted hollow nanotubes can also be loaded with certain drugs to be used as nanocarriers which can be activated by the target proteins. Furthermore, by varying the dimensions of the nanotubes, the diffusion coefficients can be controlled which is highly desired for in vivo applications.[19]

EXPERIMENTAL SECTION

Materials. The monomer 2-hydroxyethyl methacrylate (HEMA, 99%, Aldrich), the cross-linker ethylene glycol dimethacrylate (EGDMA, 98%, Aldrich), the initiator tert-butyl peroxide (TBPO, 98%, Aldrich), and 3-aminopropyltrimethoxysilane (APTS, Aldrich) are used as received. Fluorescein isothiocyanate (FITC)-labeled immunoglobulin G, lysozyme (Lyz), bovine serum albumin (BSA), 1-ethyl-3-(3-dimethylaminopropyl)carbodiimide (EDAC), and N-hydroxysuccinimide (NHS) were purchased from Sigma (St. Louis, MO). All other chemicals were of reagent grade and also purchased from Merck AG (Darmstadt, Germany) or Sigma-Aldrich Inc.

Fabrication of One-Dimensional Surface-Imprinted Polymeric Nanotubes. The AAO membranes having highly ordered nanopores were first fabricated by a previously described protocol.[21] Briefly, aluminum foil (99.99%) was first electrochemically polished using a mixture of 95 wt % H_3PO_4, 5 wt %H_2SO_4, and 20 g/L CrO_3 at 15 V for 30 min. The samples were then anodized for 12 h in a 5 wt % aqueous oxalic acid solution at 5 °C applying 50 V; a stainless steel cathode was used for the process. A thick nonuniform alumina film, which was formed across the surface of Al, was removed using a solution composed of 0.2 M CrO_3 and 0.4 M H_3PO_4 at 80 °C. To form ordered nanopores, we then carried out the second anodization using the same conditions of the first step. Afterward, AAO membranes having 93 ± 4 nm pore size, and ~9.6×10^9 pore/cm^2 were obtained with a 1 h pore opening step in 5% (v/v) of H_3PO_4 solution.

For amino modification, AAO membranes were first cleaned with deionized water and ethanol in an ultrasonic bath, and then dried on a hot plate at 150 °C for 1 h to expose the AAO−OH bonds on the pore walls. These membranes were immersed into 1% (v/v) APTS solution in ethanol. Here, APTS molecules react strongly with the free hydroxyl group of AAO−OH and resulted in the formation of Si−O−Si and AAO−O-Si bridges where methanol is the byproduct.[22] After 30 min, they were removed and sonicated in ethanol for 5 min. Finally, modified AAO membranes dried on a hot plate at 120 °C for 5 min.

The aminosilane-coupled AAO membranes were treated in an IgG solution (5 mg/mL in pH 7.4 phosphate buffer) consisting of 0.1 mg of EDAC and 0.1 mg of NHS at 4 °C for 24 h. The IgG-conjugated membranes were then washed with DI water several times and dried under the nitrogen stream.

Depositions of PHEMA films onto the IgG-conjugated nanopores of AAO are performed inside a custom-built iCVD chamber. For the fabrication of the nonimprinted nanotubes, PHEMA is also directly deposited on bare, untreated AAO templates. During depositions the chamber pressure was kept at 200 mTorr, whereas the filament temperatures were 280 °C. The flow rates of HEMA, EGDMA, and TBPO were 1.17 sccm, 0.1 and 1 sccm respectively. The overall film thickness as measured by a silicon wafer placed next to the membranes was 200 nm, which leads to a wall thickness of approximately 80 nm. After polymerization, the AAO membranes were removed from deposition chamber and immersed in 1 M HCl solution for 24h dissolving the amphoteric aluminum oxide, which was grown on the aluminum metal, resulting in open nanotube structures connected by a continuous backing of a bulk PHEMA film. To minimize collapse of the nanotubes before characterization, we first immersed samples in water for 24 h and then freeze-dried them. To obtain liberated nanotubes, we removed excess polymer from the top of AAO membrane using a scalpel, followed by polishing the membrane with a nail file. PHEMA nanotubes were freed by soaking the membrane in 1 M HCl for 24 h. Liberated nanotubes were collected from the mixture by three cycles of centrifugation (12 000 rpm, 180 s), supernatant removal, and redispersion in 1 M HCl. The procedure was followed by two cycles of centrifugation in water. The resulting polymeric nanotubes both partially etched and liberated forms were then dispersed on a silicon substrate and characterized by a QUANTA 400F field-emission scanning electron microscope (FE-SEM) with an acceleration voltage of 20 or 30 kV. The SEM images were analyzed with the freeware IMAGEJ image analysis software.

Steady-State Binding Experiments. The IgG adsorption studies with both imprinted and nonimprinted polymeric nanotubes were performed by using FITC-labeled and nonlabeled IgG through UV−vis spectrometer measurements. The liberated imprinted or non-imprinted polymeric nanotubes (~4 mg) were first placed onto a UV cuvette, and 3 mL of IgG solution (2 mg/mL in pH 7.4 buffer solution) was added into this cuvette. UV spectra of IgG solution were monitored during 24 h at room temperature, and the amount of adsorbed IgG was calculated from the calibration curves of IgG using absorbance of IgG at 495 nm for its FITC labeled form and 279 nm for its nonlabeled form. The recognition selectivity of surface-imprinted polymeric nanotubes was also evaluated by using FITC labeled and nonlabeled Lyz and BSA. Similar to IgG rebinding, both

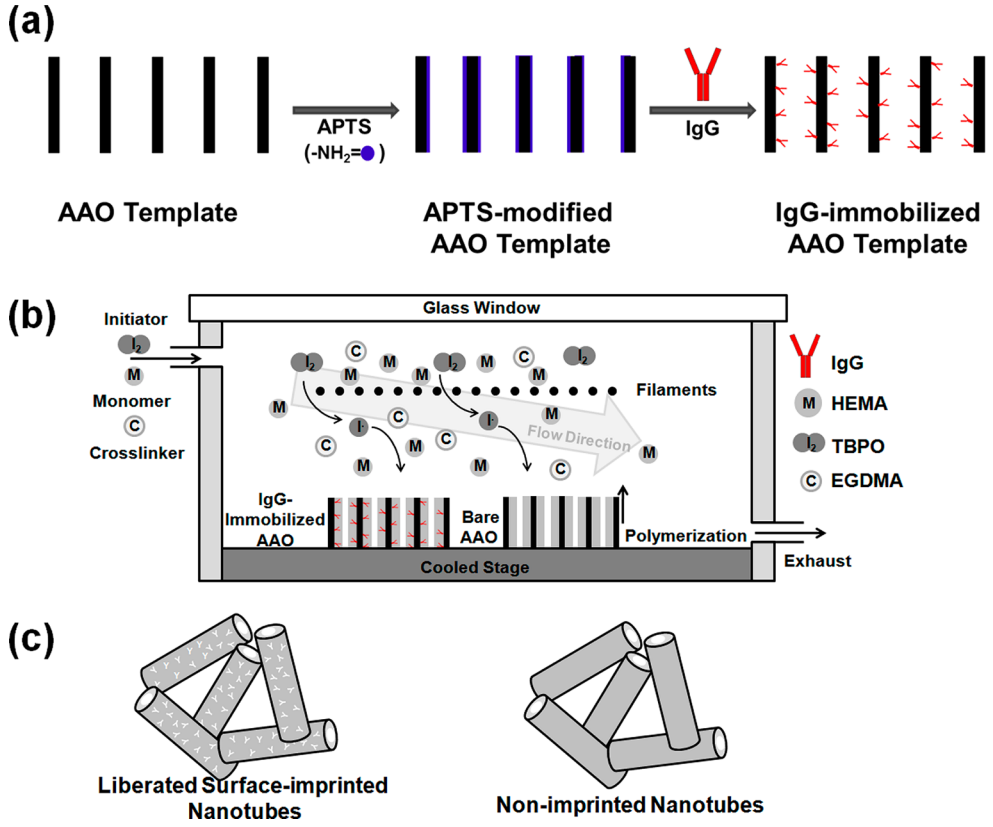

Figure 1. Schematic representation of the fabrication procedure of surface-imprinted and nonimprinted polymeric nanotubes: (a) IgG conjugation of AAO membranes, (b) polymerization inside the IgG conjugated nanopores and bare AAO by iCVD, and (c) liberated surface-imprinted and nonimprinted polymeric nanotubes.

imprinted and nonimprinted polymeric nanotubes were suspended into 3 mL of a solution of 2.0 mg/mL FITC-Lyz and FITC-BSA and allowed to equilibrate for 24 h at 4 °C in a dark place. Afterward, they were characterized by an Olympus BX51 fluorescence microscope and UV−vis spectrometer. The partition coefficients (K_d) for biomolecules showing equilibrium distribution of biomolecules between aqueous and solid phases were also calculated as $K_d = [(C_i - C_f)/C_f]V/m$, where K_d represents the partition coefficient for the biomolecules (mL/g); C_i and C_f are initial and final concentrations of biomolecules (mg/mL), respectively. V is the volume of the solution (mL) and m is the weight of the polymeric nanotubes (g). The selectivity coefficients (k) indicating the selectivity of template molecules against competitor molecules were determined by calculating the ratios of partition coefficients as $k = K_d$ (template)$/K_d$ (competitor), whereas relative selectivity coefficients (k') showing the relative selectivity gained by imprinting process were also obtained through the ratios of selectivity coefficients of imprinted and nonimprinted nanotubes as $k' = k_{imprinted}/k_{nonimprinted}$.

RESULTS AND DISCUSSION

A vapor-phase free-radical polymerization technique of iCVD was used to fabricate one-dimensional surface-imprinted polymeric nanotubes. Coating the pores of the biologically conjugated AAO membranes by iCVD and the subsequent etching of the membranes liberated the polymeric nanotubes with high binding capacity and specific recognition ability toward target molecules. The recognition ability of the nanotubes stemmed from the conjugation of the AAO membranes with the target molecules (Figure 1).

The AAO membranes, which were used as a template material in our work, were fabricated as described in the Experimental Section. Figure 2a shows the SEM image of AAO

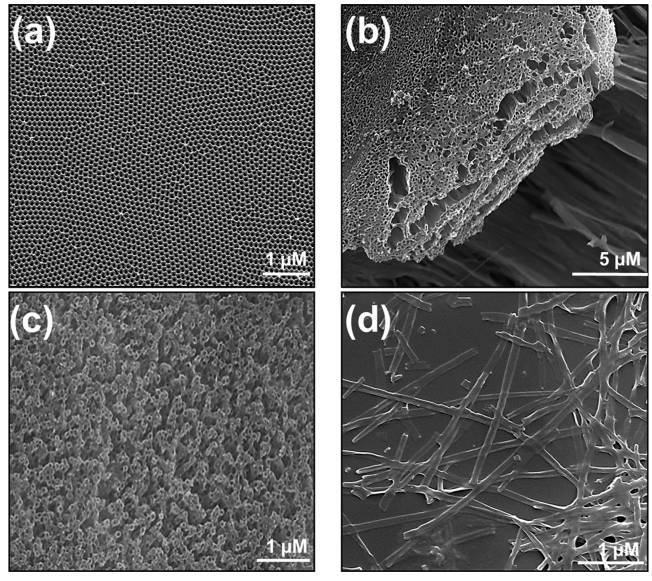

Figure 2. SEM images of (a) AAO membrane, (b, c) partially etched AAO at different magnification, and (d) liberated polymeric nanotubes dispersed on a silicon substrate.

membranes having highly monodisperse 93 ± 4 nm nanopore sizes and ~9.6 × 10^9 pore/cm^2 pore density. Afterward, they were modified with APTS resulting in the decoration of pore walls with $-NH_2$ terminal groups. The IgG molecules as a target were linked to pores through their carbonyl groups in the presence of NHS/EDAC activators (Figure 1a). The X-ray

dx.doi.org/10.1021/am401769r | ACS Appl. Mater. Interfaces 2013, 5, 6447−6452

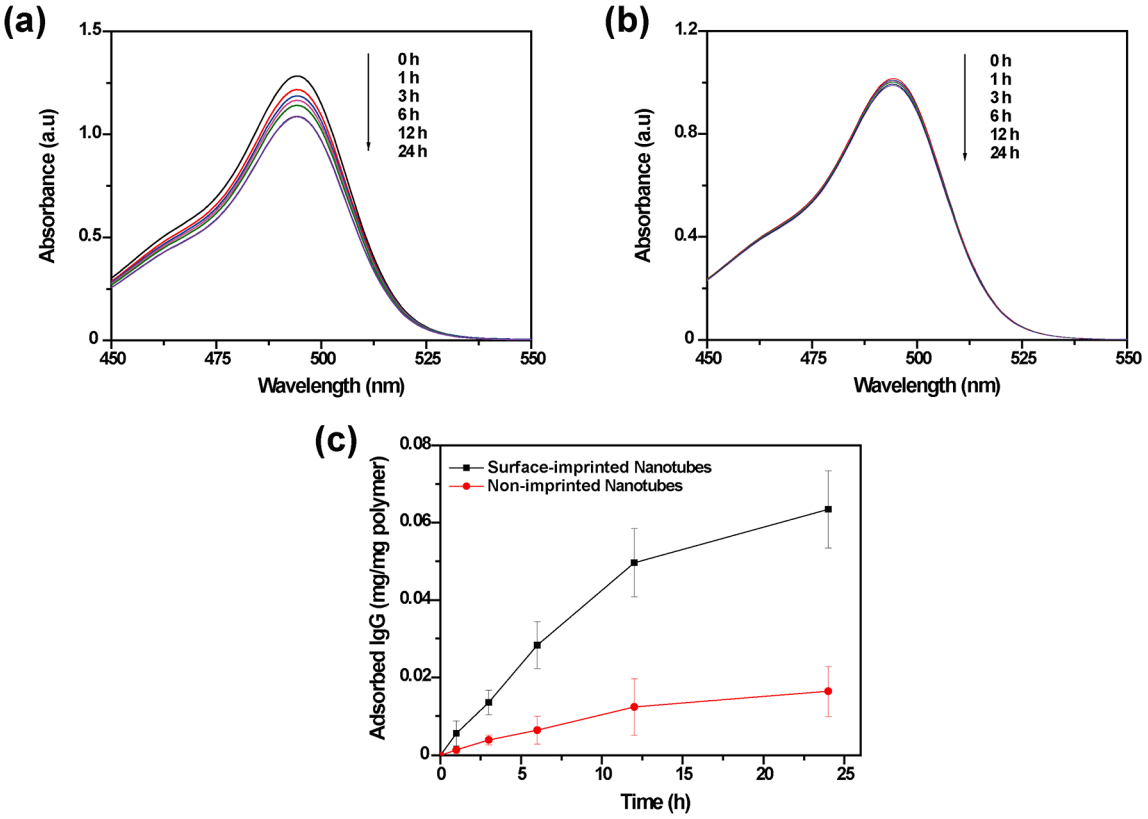

Figure 3. UV absorption spectra of FITC-IgG solution in (a) surface-imprinted polymeric nanotubes, (b) nonimprinted polymeric nanotubes, and (c) the time-dependent IgG binding plot for both imprinted and nonimprinted nanotubes.

photoelectron spectroscopy (XPS) was used for the characterization of these surfaces. For pristine AAO membrane, the binding energies of Al2p, Al2s, and O1s peaks were approximately 77, 122, and 534 eV, respectively, indicating the characteristic regions of an AAO membrane (see Figure S1A in the Supporting Information). A weak C1s peak at 293 eV was possibly due to minor hydrocarbon contamination. The XPS spectra of APTS-modified AAO surfaces also showed C (1s ~293 eV), N (1s ~401 eV), and Si (2s ~153 eV, 2p ~102 eV) peaks in addition to characteristic AAO peaks (see Figure S1B in the Supporting Information). After IgG conjugation, an obvious increment in C1s and N1s peaks was found confirming the successive IgG conjugation of AAO membranes (see Figure S1C in the Supporting Information).

The conformal coating of PHEMA hydrogels was then carried out inside the IgG conjugated nanopores by iCVD technique. Figure 1b shows the schematic of the iCVD deposition chamber under vacuum where the initiator, monomer and cross-linker vapors enter the chamber through a port and the substrates to be coated are placed on a stage kept at room temperature by the help of chillers. In the deposition process, the free-radical initiator, TBPO, was first decomposed by resistively heated filaments to form *tert*-butoxy radicals. These radicals initiated the polymerization within the pores of AAO by reacting with HEMA monomer and EGDMA cross-linker.[12] The resultant morphology of deposited polymers inside the pores of AAO membrane is tubular instead of rod because of the conformal nature of the iCVD process. By utilizing the unique advantages of the iCVD method over liquid phase deposition techniques, it is possible to control both the wall thickness of the nanotubes and physicochemical properties of the fabricated hydrogels.[12,15] Following the polymerization, AAO membranes and target molecules were subsequently removed by dilute HCl (1 M) dissolution. The SEM results (Figure 2b–d) verify the formation of polymeric nanotubes having uniform width and length indicating good replication of the original AAO structure. The chemical structures of the IgG imprinted and nonimprinted nanotubes were also confirmed by FTIR spectroscopy. For nonimprinted nanotubes, the O–H stretching vibration in PHEMA was observed in the 3600–3410 cm^{-1} range as broad absorptions. The peaks at ~1717, ~2950, and ~1250 cm^{-1} also indicated the C═O stretch mode of carbonyl groups, C–H stretching of CH_3, and C–O stretching vibration in PHEMA, respectively (see Figure S2A in the Supporting Information). The IR spectra obtained for IgG imprinted polymeric nanotubes showed weak peaks at 1635 and 1650 cm^{-1} corresponding to typical β-sheet of IgG in addition to characteristic PHEMA peaks (see Figure S2B in the Supporting Information). The amide I position at 1635 cm^{-1} found in the spectra reveals that also in imprinted IgG the β-sheet is the main structural component. The FTIR spectra indicate that there were still IgG molecules in the imprinted nanotubes after removing the template material. Therefore, the remaining imprinted IgG molecules, which may cause a negative effect on the rebinding properties of the imprinted nanotubes, were also desorbed by dispersing the nanotubes into the deionized water including sodium chloride (2%, w/v) for >2 days where the solution was replaced every 24 h. The removal of IgG was confirmed by UV spectrophotometer at 279 nm.

The IgG recognition ability of the surface-imprinted polymeric nanotubes was then evaluated by the steady-state

dx.doi.org/10.1021/am401769r | ACS Appl. Mater. Interfaces 2013, 5, 6447–6452

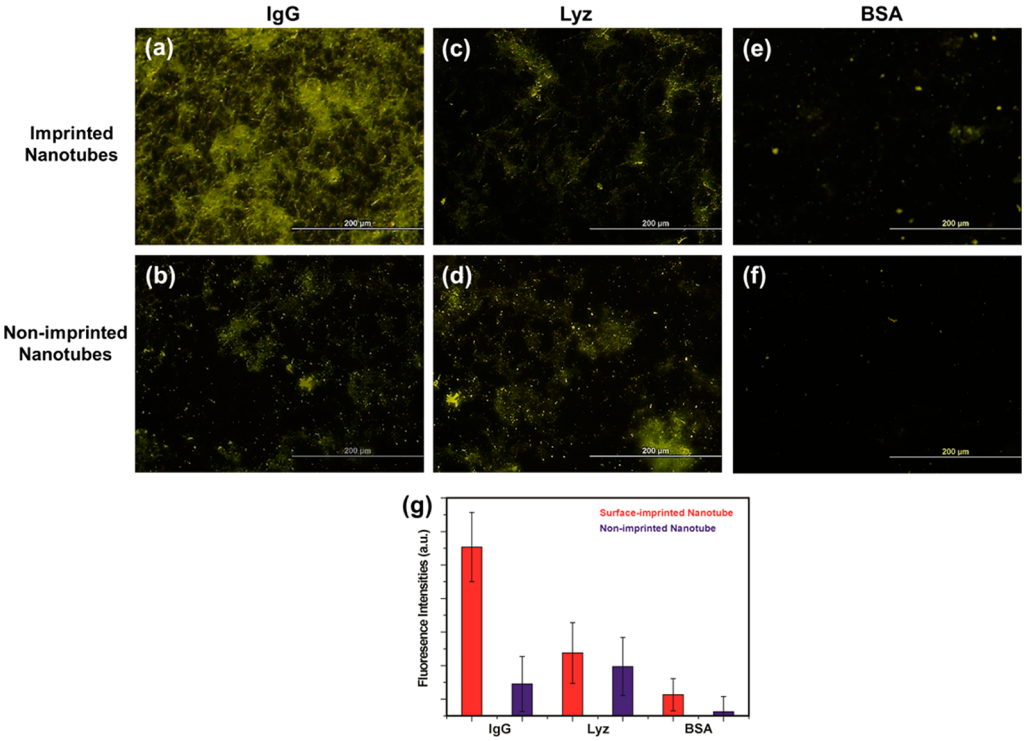

Figure 4. Fluorescence microscopy images of imprinted and nonimprinted nanotubes in the presence of (a, b) IgG, (c, d) Lyz, and (e, f) BSA. (g) Fluorescence intensities of imprinted and nonimprinted nanotubes for IgG, Lyz, and BSA, respectively.

binding method. Equal amounts of imprinted and non-imprinted nanotubes were suspended into 3 mL of FITC-IgG solution (2 mg/mL in pH 7.4 buffer solution) at room temperature in a dark place, and absorbance of the FITC-IgG solution was monitored during 24h. Once the target molecules adsorbed onto the nanotubes, a gradual decrease in the intensity of the FITC-IgG solution's at 495 nm was observed (Figure 3a, b). The time-dependent IgG adsorption for both samples was plotted in Figure 3c by means of IgG calibration curve. It is clear that the imprinted nanotubes, as expected, have a higher binding capacity (~4-fold) for IgG than those of the nonimprinted nanotubes.

This increment in binding capacity is presumably due to the high ratio of effective recognition sites, which are mainly positioned at the surface or in the proximity of the surface of nanotubes, the large surface-to-volume ratios, and the complete removal of IgG templates. Furthermore, the results also showed that in addition to the overall enhancement in the adsorbed IgG amount, the imprinted nanotubes have a significantly higher adsorption rate when compared with the nonimprinted forms possibly due to the easy diffusion of target molecules into the recognition sites on the nanotube surface and reduced mass transfer.[9,23] The adsorption rate for both cases also decreased as the adsorption process is saturated. It should be noted that similar tendencies were also observed when using unlabeled IgG molecules.

The recognition selectivity of surface-imprinted polymeric nanotubes was investigated using FITC labeled Lyz and BSA molecules. Fluorescence microscopy images and related intensity plots confirmed that the surface-imprinted polymeric nanotubes exhibit obviously the greatest affinity against IgG, followed by Lyz and BSA (Figure 4). Interestingly, we observed a significant Lyz adsorption onto both imprinted and nonimprinted nanotubes. Multilayer aggregation tendency of Lyz that does not discriminate between the nanotube types is thought to be responsible for this trend.[6] However, it should be noted that the Lyz adsorption is almost the same on both imprinted and nonimprinted polymeric nanotubes, which also indicated its nonspecific nature. Furthermore, partition coefficients (K_d), selectivity coefficients (k), and relative selectivity coefficients (k') for Lyz and BSA with respect to IgG were calculated and tabulated in Table 1.

Table 1. Partition Coefficients (K_d), Selectivity Coefficients (k), and Relative Selectivity Coefficients (k') of Lyz and BSA with Respect to IgG

	surface-imprinted		nonimprinted		
biomolecule	K_d (mL/g)	k	K_d (mL/g)	k	k'
IgG (target)	87.31		22.84		
Lyz	31.39	2.781	25.93	0.881	3.157
BSA	8.29	10.531	5.04	4.532	2.324

It is obvious that imprinted nanotubes have a greater uptake for IgG than for both Lyz and BSA whereas there is no clear tendency in the case of nonimprinted form. The k values of surface-imprinted nanotubes for IgG molecules were higher than 1.0 according to Lyz and BSA indicating that the imprinted sites have a higher specificity for target molecules meanwhile that of nonimprinted nanotubes were 0.881 for Lyz and 4.532 for BSA. The results confirmed the successive fabrication of specific cavities for IgG molecules during one-dimensional imprinting process via iCVD method. Although selectivity coefficients supply significant information about preferring target molecules to competitor, the proper coefficient to discuss the selectivity gained by imprinting process is the relative selectivity coefficient (k′) calculated by division of selectivity coefficients of imprinted to nonimprinted

dx.doi.org/10.1021/am401769r | ACS Appl. Mater. Interfaces 2013, 5, 6447−6452

polymers. These values were determined as 3.157 and 2.324 for IgG/Lyz and IgG/BSA pairs, respectively. The results showed that one-dimensional imprinted polymeric nanotubes have higher recognition ability toward target molecules, IgG, with ratios as 3.157-folds in respect to Lyz and 2.324-folds in respect to BSA, which also proved easy formation of polymeric nanotubes having higher affinity and recognition ability to target molecules by means of iCVD method.

CONCLUSION

In conclusion, we have demonstrated, for the first time, a facile method to fabricate one-dimensional surface-imprinted polymeric nanotubes by combining a biologically conjugated AAO membrane and iCVD technique for specific recognition of biomolecules. The imprinted polymeric nanotubes have relatively good monodispersity, high rebinding capacity, and significant specific recognition ability toward target molecules. As demonstrated in this work, successful iCVD applications have a great potential to circumvent the problems faced by conventional molecular imprinting approaches via utilizing its unique advantages over the liquid-based methods.

ASSOCIATED CONTENT

Supporting Information

XPS spectra of pristine AAO, APTS-modified AAO, and IgG-conjugated AAO surfaces; FTIR spectra of IgG imprinted and nonimprinted PHEMA nanotubes. This material is available free of charge via the Internet at http://pubs.acs.org.

AUTHOR INFORMATION

Corresponding Author

*E-mail: nanobiotechnology@gmail.com (G.D.); gozdeince@sabanciuniv.edu (G.O.I.).

Notes

The authors declare no competing financial interest.

REFERENCES

(1) Wulff, G. *Angew. Chem., Int. Ed.* **1995**, *34*, 1812−1832.
(2) Mosbach, K.; Ramström, O. *Nat. Biotechnol.* **1996**, *14*, 163−170.
(3) Whitcombe, M. J.; Chianella, I.; Larcombe, L.; Piletsky, S. A.; Noble, J.; Porter, R.; Horgan, H. *Chem. Soc. Rev.* **2011**, *40*, 1547−1571.
(4) Chen, L.; Xu, S.; Li, J. *Chem. Soc. Rev.* **2011**, *40*, 2922−2942.
(5) Sellergen, B.; Karmalkar, R. N.; Shea, K. J. *J. Org. Chem.* **2000**, *65*, 4009−4027.
(6) Bognar, J.; Szucs, J.; Dorko, Z.; Horvath, V.; Gyurcsanyi, R. E. *Adv. Funct. Mater.* **2013**, DOI: 10.1002/adfm.201300113.
(7) Asliyuce, S.; Uzun, L.; Say, R.; Denizli, A. *React. Funct. Polym.* **2013**, *73*, 813−820.
(8) Lee, S. B.; Mitchell, D. T.; Trofin, L.; Nevanen, T. K.; Söderlund, H.; Martin, C. R. *Science* **2002**, *296*, 2198−2200.
(9) Ouyang, R.; Lei, J.; Ju, H. *Chem. Commun.* **2008**, *44*, 5761−5763.
(10) Wang, H.; Zhou, W.; Yin, X.; Zhuang, Z.; Yang, H.; Wang, X. *J. Am. Chem. Soc.* **2006**, *128*, 15954−15955.
(11) Li, Z.; Ding, J.; Day, M.; Tao, Y. *Macromolecules* **2006**, *39*, 2629−2636.
(12) Ince, G. O.; Demirel, G.; Gleason, K. K.; Demirel, M. C. *Soft Matter* **2010**, *6*, 1635−1639.
(13) Lahann, J. *Polym. Int.* **2006**, *55*, 1361−1370.
(14) Kramer, N. J.; Sachteleben, E.; Ince, G. O.; Van De Sanden, R.; Gleason, K. K. *Macromolecules* **2010**, *43*, 8344−8347.
(15) Ince, G. O.; Coclite, A. M.; Gleason, K. K. *Rep. Prog. Phys.* **2012**, *75*, 016501.
(16) Yagüe, J. L.; Coclite, A. M.; Petruczok, C.; Gleason, K. K. *Macromol. Chem. Phys.* **2013**, *214*, 302−312.
(17) Tekin, H.; Ince, G. O.; Tsinman, T.; Gleason, K. K.; Langer, R.; Khademhosseini, A.; Demirel, M. C. *Langmuir* **2011**, *27*, 5671−5679.
(18) Ince, G. O.; Gleason, K. K.; Demirel, M. C. *Soft Matter* **2011**, *21*, 638−643.
(19) Ince, G. O.; Dubach, J. M.; Gleason, K. K.; Clark, H. A. *Proc. Natl. Acad. Sci. U.S.A.* **2011**, *180*, 2656−2661.
(20) Winther-Jensen, B.; West, K. *Macromolecules* **2004**, *37*, 4538−4543.
(21) Masuda, H.; Fukuda, K. *Science* **1995**, *268*, 1466−1468.
(22) Jani, A. M. M.; Losic, S.; Voelcker, N. H. *Prog. Mater. Sci.* **2013**, *58*, 636−704.
(23) Li, Y.; Yang, H. H.; You, A. H.; Zhuang, Z. X.; Wang, X. R. *Anal. Chem.* **2006**, *78*, 317−320.